J. Phys. D: Appl. Phys. 24 (1991) 290–300. Printed in the UK

Electron and heavy-particle kinetics in the low pressure oxygen positive column

G Gousset†, C M Ferreira‡, M Pinheiro‡, P A Sá‡, M Touzeau†, M Vialle† and J Loureiro‡

†Laboratoire de Physique des Gaz et des Plasmas (Associated with the CNRS) Université de Paris-Sud, Centre d'Orsay, 91405 Orsay Cedex, France
‡ Centro de Electrodinâmica da Universidade Técnica de Lisboa (INIC), Instituto Superior Técnico, 1096 Lisboa Codex, Portugal

Received 11 April 1990, in final form 2 October 1990

Abstract. A kinetic model for the low-pressure oxygen positive column is presented and discussed. The model is based on the electron Boltzmann equation and the rate balance equations for the dominant heavy-particle species, which are solved simultaneously in order to take into account the coupling between the electron and the heavy-particle kinetics. The effects of vibrationally excited molecules, dissociated atoms and metastable states on the electron kinetics are analysed in detail. The predicted populations of $O_2(X^3\Sigma)$, $O_2(a^1\Delta)$, $O(^3P)$, and O^- are shown to agree satisfactorily with previously reported measurements. A combination of this kinetic model with the continuity and transport equations for the charged species e, O^-, and O_2^+ is shown to provide characteristics for the maintenance field that agree reasonably well with experiment.

1. Introduction

This paper is concerned with the analysis of a kinetic model for the most populated reactive species present in the classical positive column of oxygen at low pressures, specifically $O_2(X^3\Sigma)$ and $O_2(a^1\Delta)$ molecules, $O(^3P)$ atoms and O^- ions. The present analysis is an extension of previous work in which firstly the species concentrations were measured by VUV absorption spectroscopy [1] and secondly a simplified model was developed [2] using a selected number of reactions along with electron transport and collisional data derived from swarm experiments in O_2 [3]. Although reasonable agreement was obtained between theoretical predictions and experiment, the observed discrepancies seemed, nevertheless, sufficiently important to justify further investigation.

A significant improvement achieved in the present paper is a consistent treatment of both the electron and heavy particle reaction kinetics. In fact, the electron Boltzmann equation is solved here taking into account not only the excitation and ionization of $O_2(X)$ molecules but also of $O(^3P)$ atoms, as well as the effects of electron superelastic collisions with metastables and with vibrationally excited molecules. Such processes, which are absent in a swarm experiment, can have a significant influence on the electron transport and collisional data under discharge conditions [4]. On the other hand, these electron data are necessary in order to predict the populations of the various species in the discharge. Therefore, the Boltzmann equation must be solved simultaneously with a system of rate balance equations for the various heavy particle species.

A consistent treatment of this type is also necessary to improve currently available theories of positive columns in electronegative gases, as we have shown in a recent paper [5]. Indeed, we have found that the application of the theory to the oxygen positive column, using electron transport and collisional data from swarm experiments, failed to predict accurately the maintenance field for the positive column. A possible explanation for this fact could be the changes in the electron energy distribution function caused by the various processes referred to above, as stated in [5]. This fact provides additional motivation for the analysis carried out in the present work.

In section 2 we present the Boltzmann analysis, and we investigate the effects caused by the presence of dissociated atoms and by superelastic collisions. These problems are discussed on a general basis by using the fractional concentrations of the various dominant species as parameters. In order to investigate the effects of vibrationally excited molecules, $O_2(X^3\Sigma, v)$, a characteristic vibrational temperature is also used as a parameter.

Section 3 is concerned with the heavy particle kinetics, specifically discussing the main reactions that det-

In section 4 the predicted populations as obtained by simultaneously solving the Boltzmann equation and the rate balance equations are compared to the experimental populations previously reported [1].

In section 5 we combine the present kinetic model with the continuity and the transport equations for the charged species e, O^-, and O_2^+ discussed in [5] in order to re-examine the problem of the maintenance field for the oxygen positive column.

Finally, in section 6 we present the principal conclusions of this work.

2. Electron kinetics in the oxygen positive column

2.1. Boltzmann equation

The fractional concentration of dissociated atoms in the oxygen positive column can reach very high values (~10%) under the conditions of interest here [1]. Therefore, we must treat the problem of the electron kinetics in a mixture of O_2 molecules and O atoms. Moreover, each of these species can be found in a variety of different quantum states such as, for example, $O_2(X\,^3\Sigma, v)$, $O_2(a\,^1\Delta)$, $O_2(b\,^1\Sigma)$, $O(^3P)$, $O(^1S)$, $O(^1D)$, etc. Let N denote the total gas density, N_M and N_A the total number densities of molecules and atoms, respectively, and N_{sj}, with $s = M$ or A the number density of particles of species s in the quantum state j. Let also δ represent a fractional population, defined relatively to the total density N. Then, we obviously have

$$\sum_s N_s = N_M + N_A = N; \sum_j N_{sj} = N_s;$$

$$\sum_s \delta_s = 1; \delta_M + \delta_A = 1;$$

$$\sum_j \delta_{sj} = \delta_s; \sum_{s,j} \delta_{s,j} = 1.$$

Keeping the above considerations in mind, we can write the homogeneous electron Boltzmann equation as derived from the classical two-term spherical harmonic expansion as follows:

$$-\frac{d}{du}\left[\frac{u}{3\left(\sum_s \delta_s \sigma_s\right)}\left(\frac{E}{N}\right)^2 \frac{df}{du} + \left(\sum_s \delta_s \frac{2m}{M_s}\sigma_s\right) \times u^2\left(f + \frac{KT_g}{e}\frac{df}{du}\right) + 4\delta_M B\sigma_0 uf\right] = \sum_s J_{e-s} \qquad (1)$$

where $f(u)$ is the electron energy distribution function (EEDF), normalized such that $\int_0^\infty f(u)u^{1/2}\,du = 1$, and $u = mv^2/2e$ is the electron energy expressed in electronvolts.

The three terms on the LHS of (1) represent, in order, the energy gain due to the applied field of intensity E and the energy losses due both to elastic collisions of the electrons with heavy particles of mass M_s (σ_s denotes the momentum transfer cross section for collisions of electrons with neutrals of type s; T_g is the gas temperature in Kelvin) and to rotational excitation of molecules. The latter process is treated here in the continuous approximation [6]; $B = 1.792 \times 10^{-4}$ eV is the rotational constant for O_2 and $\sigma_0 = 8\pi q^2 a_0^2/15$, where a_0 is the Bohr radius and $q = 0.29$ is the electric quadrupole moment in units of ea_0^2.

The operators J_{e-s} on the RHS of (1) represent the effects of inelastic and superelastic collisions of the electrons with the heavy species s. The explicit form of these terms is

$$J_{e-s} = \sum_{i,j} \delta_{si}[(u + V_{ij})\sigma_{si}^j(u + V_{ij})f(u + V_{ij}) - u\sigma_{si}^j(u)f(u)] + \sum_{i,j} \delta_{sj}[(u - V_{ij})\sigma_{sj}^i(u - V_{ij}) \times f(u - V_{ij}) - u\sigma_{sj}^i(u)f(u)] \qquad (2)$$

where σ_{si}^j is the electron cross section for the excitation from state i to state $j > i$; V_{ij} is the energy threshold (in eV) for this process; and σ_{sj}^i is the cross section for the reverse (superelastic) process.

As seen from equations (1) and (2), the electron kinetics is strongly coupled to the heavy particle kinetics if and when the fractional concentrations of dissociated atoms and of excited molecules or atoms become important. This is precisely the case with the oxygen positive column since large relative populations of atoms and $O_2(a\,^1\Delta)$ metastable molecules have been experimentally detected under such conditions [1].

Incidentally, the concentrations of vibrationally excited molecules $O_2(X\,^3\Sigma, v)$ and metastable states $O_2(b^1\Sigma)$, $O(^1D)$, $O(^1S)$ can also be sufficiently high so as to play a non-negligible role in the electron kinetics. For this reason we shall carry out below an analysis of the influence of the populations in various states on the electron kinetics. For the moment, this analysis will be performed using the fractional populations as independent parameters. This procedure is instructive since it enables us to identify the most significant processes and to evaluate their effects. Once this goal is achieved, we will be able to construct a self-consistent kinetic model that couples the electron and the heavy particle kinetics together (section 4).

2.2. Electron processes and cross section data

The inelastic and superelastic processes taken into account in the present work are listed in table 1 along with the pertinent references on cross section data. The cross sections for excitation of $O_2(X\,^3\Sigma, 1 \leq v \leq 4)$ and O_2 electronic states and for ionization from $O_2(X\,^3\Sigma, v = 0)$ are the same as proposed by Phelps [3]. This set is a rather complete one and provides, when inserted into the Boltzmann equation, excellent agreement between theoretical and experimental electron swarm parameters. However, additional processes must be considered under discharge conditions. For example, we also included in the model vibrational re-excitation of $O_2(X, v)$ from $1 \leq v \leq 4$ to upper-lying

Table 1. Inelastic and superelastic collision processes considered in the Boltzmann equation, and corresponding references on cross section data.

Electron processes	Reference
Molecular oxygen	
(1) $e + O_2(X, v) \rightleftarrows e + O_2(X, w)$	Phelps [3]
(2) $e + O_2(X, v = 0) \rightleftarrows e + O_2(a\,^1\Delta)$	"
(3) $e + O_2(X, v = 0) \rightleftarrows e + O_2(b\,^1\Sigma)$	"
(4) $e + O_2(X, v = 0) \rightarrow e + O_2(4.5\ eV)$	"
(5) $e + O_2(X, v = 0) \rightarrow e + O_2(6.0\ eV)$	"
(6) $e + O_2(X, v = 0) \rightarrow e + O_2(8.4\ eV)$	"
(7) $e + O_2(X, v = 0) \rightarrow e + O_2(9.97\ eV)$	"
(8) $e + O_2(X, v = 0) \rightarrow e + e + O_2^+$	"
(9) $e + O_2(X, v = 0) \rightarrow e + O_2(14.7\ eV)$	"
(10) $e + O_2(a\,^1\Delta) \rightleftarrows e + O_2(b\,^1\Sigma)$	Hall and Trajmar [25]
(11) $e + O_2(a\,^1\Delta) \rightarrow e + e + O_2^+$	(see text)
(12) $e + O_2(b\,^1\Sigma) \rightarrow e + e + O_2^+$	(see text)
Atomic oxygen	
(13) $e + O(^3P) \rightleftarrows e + O(^1D)$	Henry *et al* [26]
(14) $e + O(^3P) \rightleftarrows e + O(^1S)$	"
(15) $e + O(^3P) \rightarrow e + O(^3S)$	Stone and Zipf [27]
(16) $e + O(^1D) \rightleftarrows e + O(^1S)$	Henry *et al* [26]
(17) $e + O(^3P) \rightarrow e + e + O^+$	Fite and Brackmann [28]
(18) $e + O(^1D) \rightarrow e + e + O^+$	Drawin [7]
(19) $e + O(^1S) \rightarrow e + e + O^+$	"

vibrational levels $w \leqslant v + 4$. The cross sections for such processes are unknown and they were assumed here to be the same as those for the transitions $O_2(X, 0 \rightarrow w - v)$ but with the threshold appropriately shifted due to the anharmonicity of the molecular vibration. The reverse processes, i.e. superelastic collisions producing vibrational de-excitation, were also taken into account. The model also includes the following: superelastic de-excitation of $O_2(a\,^1\Delta)$ and $O_2(b\,^1\Sigma)$ to the ground state as well as transitions between these states and their ionization (assuming the cross section to be the same as for ionization from the ground state but with the appropriate shift in the threshold); excitation of the atomic states $O(^1D)$, $O(^1S)$, $O(^3S)$ and ionization from ground state $O(^3P)$ atoms; ionization from $O(^1D)$ and $O(^1S)$ (using cross sections calculated according to Drawin's formula [7]); transitions between $O(^1D)$ and $O(^1S)$; and superelastic de-excitation of both of these states to the ground state $O(^3P)$. All the cross sections for superelastic processes have been determined from those for the direct processes by detailed balancing.

We note that the above list of electronic processes implies that the solutions to the Boltzmann equation depend on the fractional populations, δ_{sj}, of the following species: $O_2(X\,^3\Sigma,\ 0 \leqslant v \leqslant 8)$; $O_2(a\,^1\Delta)$; $O_2(b\,^1\Sigma)$; $O(^3P)$; $O(^1D)$; $O(^1S)$. In practice, for lack of data we cannot take into account electronic excitation and ionization of O_2 from $O_2(X\,^3\Sigma, v > 0)$. Therefore, we have dealt with such processes as if they only occurred from the $v = 0$ level but assuming in this case that all the $O_2(X\,^3\Sigma)$ state population is in that level. In other words, the distribution of $O_2(X\,^3\Sigma)$ molecules among various vibrational levels only was taken into account when dealing with vibrational excitation or de-excitation processes within the ground electronic state. Since no attempts were made in this work to model the vibrational kinetics of O_2 we shall assume in the following that the vibrational distribution can be characterized by a vibrational temperature whose meaning is explained below.

2.3. Vibrational distribution function of $O_2(X^3\Sigma, v)$ molecules

We represent the intermolecular potential by an anharmonic Morse oscillator whose energy levels are given by

$$E_v = \hbar\omega_e[(v + \tfrac{1}{2}) - \chi_e(v + \tfrac{1}{2})^2] \qquad (3)$$

where for $O_2(X\,^3\Sigma)$, $\omega_e = 1580.19\ cm^{-1}$ and $\omega_e\chi_e = 11.98\ cm^{-1}$ [8, 9]. We assume that the vibrational distribution function has the form proposed by Gordiets *et al* [10], namely

$$N_v = N_0 \exp\left\{-v\left[\frac{\Delta E_{1,0}}{KT_V} - (v-1)\frac{\chi_e\theta}{T_g}\right]\right\} \qquad v \leqslant v^* \qquad (4)$$

$$N_v = N_{v^*}\frac{v^*}{v} \qquad v^* \leqslant v \leqslant v^{**} \qquad (5)$$

and $N_v \sim \exp(-\Delta E_v/KT_g)$ for $v > v^{**}$. Here, N_v denotes the number density of molecules in level v; $\Delta E_{1,0} = \hbar\omega_e(1 - 2\chi_e)$ is the energy difference between the levels $v = 1$ and $v = 0$; $\theta = \hbar\omega_e/K = 2270.73\ K$; T_V is the characteristic vibrational temperature; and v^* is the vibrational quantum number corresponding to the

Table 2. List of cases considered in the parametric study of the solutions to the Boltzmann equation of section 2 (see main text for notation).

Case	T_V (K)	δ_{MX}	δ_{Ma}	δ_{Mb}	δ_{AP}	δ_{AD}	δ_{AS}
A	300	1	0	0	0	0	0
B	300	0.72	0.18	0	0.10	0	0
C	2000	0.72	0.18	0	0.10	0	0
D	2000	0.64	0.16	0	0.20	0	0
E	300	0.879	4.65×10^{-2}	4.65×10^{-3}	7.0×10^{-2}	2.6×10^{-5}	1.0×10^{-6}
F	300	0.765	0.121	1.3×10^{-2}	0.10	1.0×10^{-4}	1.0×10^{-5}

minimum of the Treanor distribution [11] (equation (4)) given by

$$v^* = \tfrac{1}{2}\left(1 + \frac{\Delta E_{1,0}}{KT_V}\frac{T_g}{\chi_e \theta}\right). \tag{6}$$

For the conditions considered here ($T_V \leqslant 3000$ K; $T_g < 700$ K) only the Treanor-like region (equation (4)) and the plateau region (equation (5)) have any relevance in what concerns the effects on the electron kinetics. In the following we shall assume $T_g = 300$ K and we shall investigate the effects of the parameter T_V by considering two extreme situations: $T_V = 300$ K and $T_V = 2000$ K. However, the experimental values of T_g will be used in the calculations of section 4.

2.4. Electron transport parameters and rate coefficients

The various combinations of independent parameters T_V and δ_{sj} considered in the present analysis are listed in table 2, where the subscripts to δ refer to the following molecular and atomic states: δ_{MX}, $O_2(X\,^3\Sigma)$; δ_{Ma}, $O_2(a\,^1\Delta)$; δ_{Mb}, $O_2(b\,^1\Sigma)$; δ_{AP}, $O(^3P)$; δ_{AD}, $O(^1D)$; δ_{AS}, $O(^1S)$. In all cases $T_g = 300$ K.

Case A corresponds to the so-called molecular cold gas approximation in which the electrons can be assumed to collide only with ground state molecules, $O_2(X\,^3\Sigma, v = 0)$. This is the case considered by Masěk *et al* [12] and Láska *et al* [13] in their previous analysis of the oxygen positive column, and also by Phelps [3] in his Boltzmann analysis of electron swarms in O_2. We have checked that our Boltzmann code reproduces Phelps's macroscopic data (transport parameters and rate coefficients) to within a few per cent, in this case. Case B is intended to analyse the effects caused by the presence of $O(^3P)$ atoms and by superelastic collisions with metastable $O_2(a\,^1\Delta)$ molecules, using realistic values for the relative concentrations of these species [1]. In case C we additionally consider the effects of vibrationally excited molecules, assuming a relatively high degree of vibrational excitation. Present experimental evidence indicates that $T_V \sim T_g$ (see below) so that case C should be regarded only as an extreme situation of vibrational excitation. Case D is also an extreme situation in what concerns the presence of dissociated atoms. Finally, cases E and F investigate the effects caused by collisions with the various molecular and atomic metastable states, using realistic values for their relative concentrations. The latter two cases should be regarded as the most realistic ones.

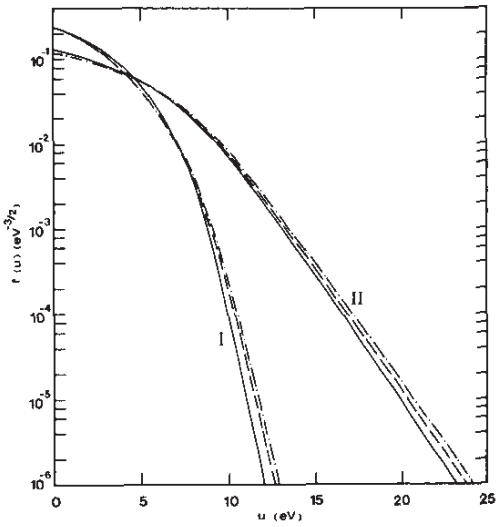

Figure 1. Electron energy distribution function for $E/N = 3 \times 10^{-16}$ V cm^2 (I) and 10^{-15} V cm^2 (II), and for the following cases considered in table 2: A, full curve; C, broken curve; D, chain curve.

Figure 1 shows the EEDF obtained in cases A, C and D, for $E/N = 30$ and 100 Td (1 Td = 10^{-17} V cm^2). We note that there is a small enhancement in the tail of the distribution in cases C and D compared with case A. This enhancement is principally caused by superelastic collisions at low E/N and by the presence of $O(^3P)$ atoms at high E/N. The computed EEDF for case A can be compared to Langmuir probe measurements by Rundle *et al* [14] in a discharge tube of 1.26 cm diameter for pressures 0.5–3 torr and currents 1–10 mA. Under such experimental conditions the concentrations of atoms and excited molecules are indeed too small to affect the EEDF. The measurements of Rundle *et al* [14] were found to agree well with the calculations of Hake and Phelps [15] which in turn also agree with our calculations for case A (apart from small differences caused by re-adjustments made in cross section data from [15] to [3]).

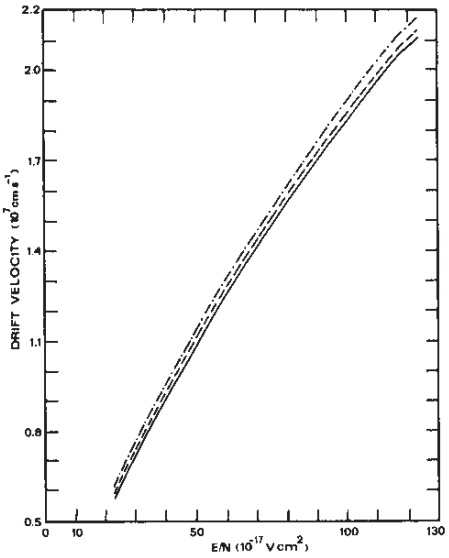

Figure 2. Electron drift velocity as a function of E/N for the same cases A, C and D as in figure 1.

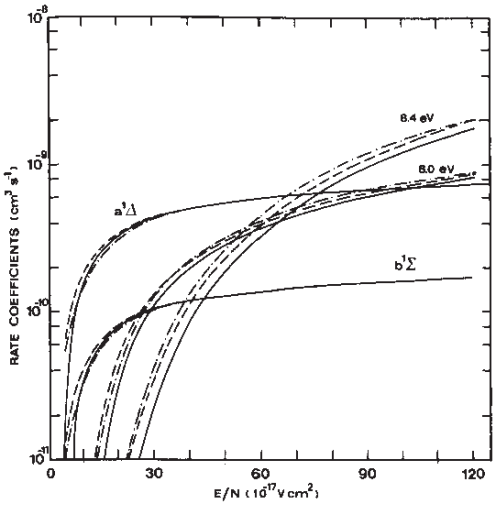

Figure 4. Electron rate coefficients as a function of E/N for the same cases as in figures 2 and 3: excitation of the states a $^1\Delta$ and b $^1\Sigma$, and 6.0 and 8.4 eV energy loss processes.

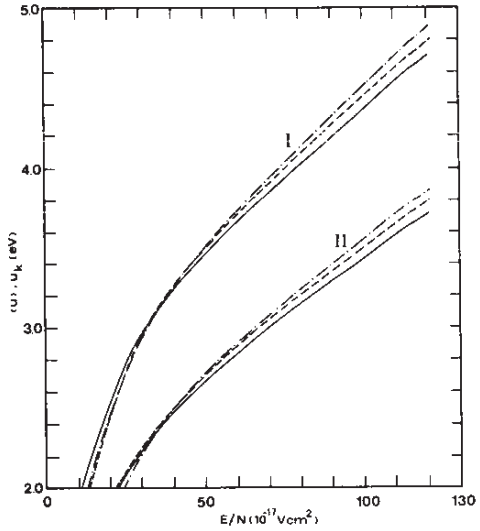

Figure 3. Electron mean energy (I) and characteristic energy (II) as a function of E/N for the same cases as in figure 2.

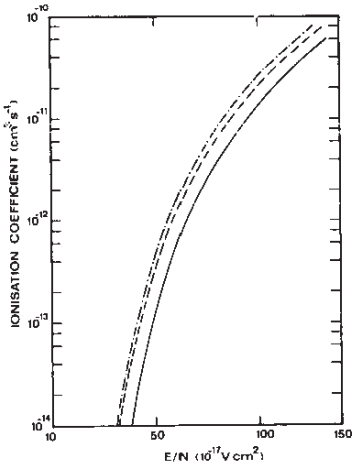

Figure 5. Total electron rate coefficient for ionization as a function of E/N for the same cases as in figures 2–4.

Figures 2–5 show various electron transport parameters and rate coefficients obtained in the same three cases as above. The effects of superelastic collisions and dissociation on the electron drift velocity (figure 2), average energy and characteristic energy (figure 3) are small but tend to increase with E/N. Such effects are, however, more important at low E/N for the excitation rate coefficients shown in figure 4. Figure 5 shows the total rate coefficient for ionization, including in cases C and D the contributions of ionization from $O_2(X\,^3\Sigma)$, $O_2(a\,^1\Delta)$ and $O(^3P)$. These contributions, which are weighted according to the relative populations in these states, are shown in figure 6 for case C. Compared with case A, the total

at the lower E/N values and by a factor of 1.5–2 at E/N = 100 Td.

Figure 7 shows the electron percentage energy losses as a function of E/N in cases A and C. In order to evaluate the respective effects of $O_2(a\,^1\Delta)$ and $O(^3P)$, also shown in this figure are curves obtained by setting $\delta_{AP} = 0$ and keeping the ratio $[O_2(a\,^1\Delta)]/[O_2(X\,^3\Sigma)]$ the same as in case C.

A detailed numerical analysis of cases E and F reveals that the presence of the small (but realistic) populations in the states $O_2(b\,^1\Sigma)$, $O(^1S)$ and $O(^1D)$ considered in table 2 has a negligible effect on the electron kinetics. Therefore, it appears that only the presence of vibrationally excited molecules (at high T_V), $O_2(a\,^1\Delta)$ metastables and $O(^3P)$ atoms may affect

DOCKET ALARM

Explore Litigation Insights

Docket Alarm provides insights to develop a more informed litigation strategy and the peace of mind of knowing you're on top of things.

Real-Time Litigation Alerts

Keep your litigation team up-to-date with **real-time alerts** and advanced team management tools built for the enterprise, all while greatly reducing PACER spend.

Our comprehensive service means we can handle Federal, State, and Administrative courts across the country.

Advanced Docket Research

With over 230 million records, Docket Alarm's cloud-native docket research platform finds what other services can't. Coverage includes Federal, State, plus PTAB, TTAB, ITC and NLRB decisions, all in one place.

Identify arguments that have been successful in the past with full text, pinpoint searching. Link to case law cited within any court document via Fastcase.

Analytics At Your Fingertips

Learn what happened the last time a particular judge, opposing counsel or company faced cases similar to yours.

Advanced out-of-the-box PTAB and TTAB analytics are always at your fingertips.

API

Docket Alarm offers a powerful API (application programming interface) to developers that want to integrate case filings into their apps.

LAW FIRMS
Build custom dashboards for your attorneys and clients with live data direct from the court.

Automate many repetitive legal tasks like conflict checks, document management, and marketing.

FINANCIAL INSTITUTIONS
Litigation and bankruptcy checks for companies and debtors.

E-DISCOVERY AND LEGAL VENDORS
Sync your system to PACER to automate legal marketing.